

---

# Navigating loss manifolds via rigid body dynamics: A promising avenue for robustness and generalisation

---

**Mohammed D. Belgoumri**  
Deakin University  
[m.belgoumri@deakin.edu.au](mailto:m.belgoumri@deakin.edu.au)

**Mohamed Reda Bouadjenek**  
Deakin University  
[reda.bouadjenek@deakin.edu.au](mailto:reda.bouadjenek@deakin.edu.au)

**Hakim Hacid**  
Technology Innovation Institute  
[Hakim.Hacid@tii.ae](mailto:Hakim.Hacid@tii.ae)

**Imran Razzak**  
Mohamed bin Zayed University  
of Artificial Intelligence  
[imran.razzak@mbzuai.ac.ae](mailto:imran.razzak@mbzuai.ac.ae)

**Sunil Aryal**  
Deakin University  
[sunil.aryal@deakin.edu.au](mailto:sunil.aryal@deakin.edu.au)

## Abstract

Training large neural networks through gradient-based optimization requires navigating high-dimensional loss landscapes, which often exhibit pathological geometry, leading to undesirable training dynamics. In particular, poor generalization frequently results from convergence to sharp minima that are highly sensitive to input perturbations, causing the model to overfit the training data while failing to generalize to unseen examples. Furthermore, these optimization procedures typically display strong dependence on the fine structure of the loss landscape, leading to unstable training dynamics, due to the fractal-like nature of the loss surface. In this work, we propose an alternative optimizer that simultaneously reduces this dependence, and avoids sharp minima, thereby improving generalization. This is achieved by simulating the motion of the center of a ball rolling on the loss landscape. The degree to which our optimizer departs from the standard gradient descent is controlled by a hyperparameter, representing the radius of the ball. Changing this hyperparameter allows for probing the loss landscape at different scales, making it a valuable tool for understanding its geometry.

## 1 Introduction

Training modern Deep Learning (DL) models boils down to solving high-dimensional optimization problems, where the objective is to minimize a non-convex loss function defined over millions or even billions of parameters. The dominant approach to solving these problems relies on gradient-based optimizers like Stochastic Gradient Descent (SGD) [1], which iteratively updates model parameters using noisy estimates of the gradient. Because these optimizers rely on local pointwise information about the loss function and its derivatives, they are unable to account for the global structure of the loss landscape. In the context of complex neural loss landscapes, which present challenging geometries [2–4], such as sharp minima [5, 6] and saddle points with large indices [7], this leads to poor generalization and optimization dynamics.

Multiple works have attempted to address these issues by introducing novel optimizers designed to handle these problematic geometries, particularly the presence of sharp minima. A common strategy among these approaches is to incorporate global information about the loss landscape to guide optimization more effectively. Sharpness-Aware Minimization (SAM) [8] is one such optimizer, which attempts to avoid sharp minima by adding a sharpness penalty to the loss function, making them less attractive. Entropy-SGD [9] is another example of a sharpness-avoiding optimizer, which works by optimizing over a smoothed version of the loss function. Both SAM and Entropy-SGD look at the values of the loss function on an entire open domain around an iterate to compute the next one [8, 9]. The ubiquity of this strategy is not due to chance, rather it is a necessary condition for an optimizer to have some robustness to loss landscape geometry. The intuition for this claim is that a completely local (point-like) optimizer’s trajectory can be influenced by arbitrarily small formations in the loss landscape, meaning that arbitrarily sharp and ill-conditioned valleys can capture the iterates. We argue that purely local optimization methods suffer from two fundamental limitations: (i) their strong reliance on infinitesimal features of the loss landscape makes them inherently prone to overfitting due to excessive sensitivity to data-dependent irregularities; and (ii) inability to explore, as their point-like nature causes them to almost immediately fall into a nearby local minimum, limiting the distance they are able to travel [10].

To address the problems outlined above, this paper takes a closer look at the contrast between local and global optimization methods. Specifically, we propose to replace the point-like dynamics of standard optimizers with those of a rigid body with finite size. Such dynamics are invariant to changes in the loss landscape geometry below a certain characteristic scale, defined by the intrinsic size of the moving object. Therefore, the optimizer is only affected by the “*macroscopic*” features of the loss landscape, which are much less sensitive to data noise or other hazards such as poisoning attacks. To illustrate this concept, we take the case of a ball rolling on a surface in which the dynamics can be simplified by focusing on the center’s motion reducing them to those of a point particle under a distance constraint. We show that these dynamics depend only on a small region of the loss landscape (which gets smaller as the radius of the ball increases). Furthermore, we identify a critical radius below which the optimizer behaves as standard SGD. Finally, we empirically show that the radius hyperparameter provides an explicit control over the trade-off between exploration and exploitation.

## 2 Preliminaries

Throughout this paper, we consider the typical DL training setup of minimizing a positive ( $k$  times continuously) differentiable loss function  $f : \mathbb{R}^d \rightarrow \mathbb{R}$ ,  $d$  being the parameter space dimension. The graph of  $f$ , i.e., the set  $\Gamma = \{(\theta, f(\theta)) \mid \theta \in \mathbb{R}^d\}$ , is a ( $C^k$ ) smooth  $d$ -dimensional submanifold of  $\mathbb{R}^d \times \mathbb{R} \cong \mathbb{R}^{d+1}$ . We refer to  $\Gamma$  as the *loss manifold*, *loss surface*, or *loss landscape*, to  $\mathbb{R}^d$  as the *parameter space*, and to  $\mathbb{R}^{d+1}$  as the *ambient space*.  $\Gamma$  is naturally parametrized by the mapping  $\theta \mapsto (\theta, f(\theta))$ , which defines a  $C^k$ -diffeomorphism between  $\mathbb{R}^d$  and  $\Gamma$ .  $\Gamma$  is therefore orientable, and thus admits a continuous unit normal vector field  $\nu$  given by

$$p = (\theta, f(\theta)) \mapsto \nu(p) = \frac{1}{\sqrt{1 + \|\nabla f(\theta)\|^2}} \begin{bmatrix} -\nabla f(\theta) \\ 1 \end{bmatrix}, \quad (1)$$

On account of its smoothness,  $\Gamma$  also admits a continuous tangent vector field  $\tau$  given by

$$p = (\theta, f(\theta)) \mapsto \tau(p) = \begin{bmatrix} \nabla f(\theta) \\ \|\nabla f(\theta)\|^2 \end{bmatrix}. \quad (2)$$

### 2.1 Offset manifolds and tubular neighborhoods

For any point  $p \in \mathbb{R}^{d+1}$ , the distance of  $p$  to  $\Gamma$  is defined as

$$d_\Gamma(p) = \inf_{q \in \Gamma} \|p - q\| \quad (3)$$

The sublevel sets of the function  $d_\Gamma$  are referred to as *tubular neighborhoods* of  $\Gamma$ . More precisely, for  $\rho > 0$ , the  $\rho$ -tubular neighborhood of  $\Gamma$  is the set

$$d_\Gamma^{-1}([0, \rho]) := \left\{ p \in \mathbb{R}^{d+1} \mid d_\Gamma(p) < \rho \right\}, \quad (4)$$

or equivalently, the set

$$\bigcup_{p \in \Gamma} B(p, \rho), \quad (5)$$

where  $B(p, \rho)$  is the open ball of radius  $\rho$  centered at  $p$  [11]. The boundary of the tubular neighborhood, or equivalently the level set  $d_\Gamma^{-1}(\{\rho\})$ , is referred to as the  $\rho$ -*offset manifold* of  $\Gamma$ , and is denoted by<sup>1</sup>  $\Gamma_\rho$ . It is easy to see that  $\Gamma_\rho$  is also a  $d$ -dimensional submanifold of  $\mathbb{R}^{d+1}$ , and that it is  $\mathcal{C}^k$ -diffeomorphic to  $\Gamma$  for small enough  $\rho$  [11].

## 2.2 Projecting onto a manifold

Since  $\Gamma$  is closed, for any point  $p \in \mathbb{R}^{d+1}$ , there exists a point  $q \in \Gamma$  such that  $\|p - q\| = d_\Gamma(p)$ . The set of all such points is called the *projection* of  $p$  onto  $\Gamma$ , denoted by  $\text{proj}_\Gamma(p)$  [11, 12]. The set of points  $p \in \mathbb{R}^{d+1}$  such that  $\text{proj}_\Gamma(p)$  has at least two elements is called the *medial axis* of  $\Gamma$  [11, 12]. Using the projection operator on the updates or iterates of gradient descent, we obtain a new algorithm whose iterates are confined to a certain manifold (typically, an offset of  $\Gamma$ ). This algorithm is referred to as Projected Gradient Descent (PGD) [13].

## 3 Rolling ball optimizer

In the continuous time limit, most gradient-based optimizers have limiting dynamics of the form  $\dot{\theta} = F(\theta)$ , or  $\ddot{\theta} = F(\theta, \dot{\theta})$  in the case of momentum-based optimizers, where  $F$  is some transfer function. In both cases, the dynamics are point-like, and depend only on the local geometry of the loss landscape. That is, adding a small globally bounded perturbation to the loss landscape (e.g., by introducing noise in the data), or slightly changing the initialization of the optimizer, can lead to unrecognizable changes in the trajectory, and therefore in the final model. Such optimizers are therefore inherently susceptible to overfitting.

### 3.1 Proposed algorithm

---

**Algorithm 1:** Rolling ball optimizer

---

**Input:** Loss function  $f : \mathbb{R}^d \rightarrow \mathbb{R}$   
 Learning rate  $\eta > 0$   
 Ball radius  $\rho > 0$   
 Initial solution  $\theta_0 \in \mathbb{R}^d$   
 Number of epochs  $n_{\text{epochs}} \geq 1$

```

1 begin
2    $p_0 \leftarrow (\theta_0, f(\theta_0))$ 
3   for  $t = 0$  to  $n_{\text{epochs}}$  do
4      $c_t \leftarrow \theta + \rho \nu(p_t)$ 
5      $\tilde{c}_{t+1} \leftarrow c_t - \eta \tau(p_t)$ 
6      $p_{t+1} \leftarrow \text{proj}_\Gamma \tilde{c}_{t+1}$ 
7   end
8 end
```

**Output:** Optimal solution  $\theta^*$

---

<sup>1</sup>In reality, the boundary has two connected components, one of which is above the loss landscape. We will denote it by  $\Gamma_\rho$ , and refer to it, by abuse of language, as the  $\rho$ -*offset* of  $\Gamma$ .

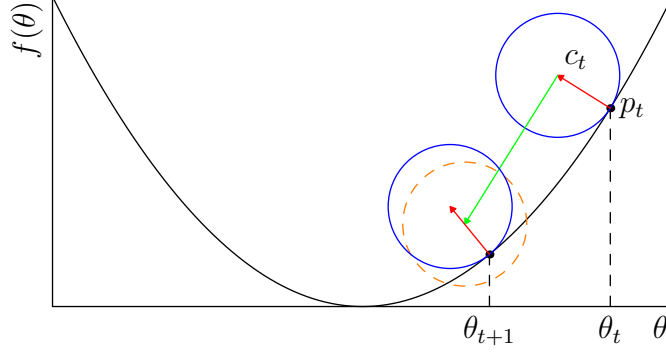


Figure 1: One update step of the rolling ball optimizer.

We identify the point-like nature of standard optimizers as the root cause of many of their inadequacies. To address them, we propose to replace the point particle with a ball of finite radius  $\rho$  rolling on the loss landscape, while – crucially – maintaining tangential contact with  $\Gamma$  (See Figure 1). Discretizing the temporal dynamics of the ball’s center yields a non-local optimizer, that naturally generalizes its gradient-based counterpart.

To derive the update rule for the rolling ball analog of gradient descent, consider time step  $t$ , at which the ball is tangent to  $\Gamma$  at point  $p_t = (\theta_t, f(\theta_t))$ . The center of the ball is given by

$$c_t = p_t + \rho\nu(p_t). \quad (6)$$

To update the ball’s position, we allow the center to move in the steepest descent direction of  $\Gamma$ , simulating a downwards force applied at  $c_t$ . This results in a *candidate* center  $\tilde{c}_{t+1}$  given by

$$\tilde{c}_{t+1} = c_t - \eta\tau(p_t), \quad (7)$$

where  $\eta$  is the learning rate. This, most likely, violates the tangency constraint, as  $\rho$ -ball around  $\tilde{c}_{t+1}$  probably intersects  $\Gamma$  (as shown in Figure 1). In order to fix this, we need to handle the “collision” by projecting the candidate center onto  $\Gamma$ , resulting in the footpoint  $p_{t+1}$ :

$$p_{t+1} = \text{proj}_{\Gamma}(\tilde{c}_{t+1}). \quad (8)$$

For the purposes of this paper, we assume oracle access to  $\text{proj}_{\Gamma}$ , which in practice, reduces to solving an optimization problem (see Section 2.2). For the purpose of experimentation, we opt for a naive implementation of  $\text{proj}_{\Gamma}$ , using an iterative optimizer (in fact, a gradient-based optimizer, see Section 5).

The pseudocode for this method is given in Algorithm 1. Either the sequence  $(p_t)_{t \geq 0}$  or  $(c_t)_{t \geq 0}$  can be taken as the *trajectory* of the Rolling Ball Optimizer (RBO). Their projection  $(\theta_t)_{t \geq 0}$  onto the parameter space  $\mathbb{R}^d$  are the iterates of the optimizer. In particular,  $\theta_{n_{\text{epochs}}}$  is the learned parameter vector.

### 3.2 Distance constraint projection

Instead of footpoint projection, a distance projection can be applied directly to the update. Consider the loss landscape distance function given by Equation (3). Algorithm 1 has the (approximate) invariant

$$\forall t \geq 0, \quad d_{\Gamma}(c_t) = \rho \quad (9)$$

The update rule is given by Equation (7) uses an adjustment

$$\tilde{\delta}_t = -\eta\tau(p_t), \quad (10)$$

the application of which violates Equation (9). This can be remedied by projecting  $\tilde{\delta}_t$  onto the orthogonal complement of  $u = \nabla d_{\Gamma}(c_t)$

$$\delta_t = \tilde{\delta}_t - \frac{\langle u, \tilde{\delta}_t \rangle}{\|u\|^2} u. \quad (11)$$

This allows us to compute the next center directly as

$$c_{t+1} = c_t + \delta_t. \quad (12)$$

It is easy to verify that this implementation verifies the same approximate invariant as Algorithm 1.

## 4 Theoretical analysis

The main claim of this paper is that rolling ball optimizers are less sensitive to the fine-grained topography of the loss landscape. In this section, we formulate and prove a rigorous version of this claim. The fundamental assumption we will be using is that the invariant in Equation (9) holds. This is equivalent to the assumption that  $c_t$  is confined to  $\Gamma_\rho$ , the (upper)  $\rho$  offset of  $\Gamma$ , or that  $p_t$  is confined to the set of “ $\rho$ -reachable points” of  $\Gamma$  (see Definition 1). Intuitively, a point  $p \in \Gamma$  is unreachable by a ball of radius  $\rho > 0$  if and only if, all balls of radius  $\rho$  that touch  $p$ , go through  $\Gamma$ . It should be noted that the assumption of Equation (9) does not hold exactly in practice. However, it holds in the continuous time limit of Algorithm 1.

### 4.1 Unreachable points

**Definition 1** (Unreachable point).

A point  $p \in \Gamma$  is said to be  $\rho$ -unreachable ( $\rho > 0$ ) if and only if for all possible centers  $c \in \mathbb{R}^d \times \mathbb{R}$ ,

$$\|c - p\| = \rho \implies \exists q \in \Gamma, \|c - q\| < \rho.$$

The existence of unreachable points is a key distinguishing feature of rolling ball optimizers compared to gradient descent optimizers. It is the inability of the ball to penetrate into microscopic valleys that makes it invariant to their topography. This is more-or-less identical to the intuition behind the rolling ball method from image processing [14].

Given their central role in the robustness of our optimizer, it stands to reason that understanding unreachable points is necessary to understand the optimizer’s behavior. Two (rather intuitive) properties of the set of unreachable points are:

- (i) if it contains a point  $p$ , then it contains all points within a certain distance  $\rho$  of  $p$ , i.e., it is open (in the topology of  $\Gamma$ , see Lemma 1), and
- (ii) it grows as the radius increases.

In fact, not only does the set of unreachable points grow, in the limit as  $\rho \rightarrow +\infty$ , it contains all points in  $\Gamma$  that are not local maxima.

**Lemma 1** (Non-isolated unreachable points).

*If  $p \in \Gamma$  is an  $\rho$ -unreachable point for some  $\rho > 0$ , then there exists  $\varepsilon > 0$  such that all points in  $B(p, \varepsilon)$  are  $\rho$ -unreachable.*

*Proof.*

Let  $U = \bigcup_{q \in \Gamma} B(q, \rho)$  be the  $\rho$ -tubular neighborhood of  $\Gamma$ , and let  $E = \mathbb{R}^{d+1} \setminus U$ . One shows with ease that  $p \in \mathbb{R}^{d+1}$  is  $\rho$ -unreachable if and only if  $S(p, \rho) \subset U$ .

Let  $p \in \Gamma$  be an  $\rho$ -unreachable point, and let  $S = S(p, \rho)$ . The distance

$$d(S, E) = \inf \{ \|x - y\| \mid x \in S \wedge y \in E \} > 0,$$

since if  $d(S, E) = 0$ , then  $S \cap E \neq \emptyset$ , because  $S$  is compact and  $E$  is closed, contradicting the  $\rho$ -unreachability of  $p$ .

Defining  $\varepsilon = \delta/2$ , let  $p' \in B(p, \varepsilon)$ ,  $a$  be an arbitrary point on  $S' := S(p', \rho)$ , and  $s = a + p - p'$ .

One verifies with ease that  $s \in \mathcal{S}$ , since

$$\|p - s\| = \|p' - a\| = \rho,$$

and that

$$\|a - s\| = \|p - p'\| < \varepsilon.$$

Therefore,  $d(a, \mathcal{S}) < \varepsilon$ , which implies that  $a \in U$ . Since  $a$  was chosen arbitrarily on  $\mathcal{S}'$ , it follows that  $\mathcal{S}' \subset U$ , which means that  $p'$  is  $\rho$ -unreachable.

□

## 4.2 The ironing property

A second important property of the RBO (which is also a result of the properties of offset manifolds) is the *ironing property*. Loosely speaking, as the radius increases, the shape of the loss landscape is smoothed (see Figure 3). In particular, for a global flat (i.e., bounded) loss function landscape, one would expect the offset manifold to approach a horizontal hyperplane as  $\rho \rightarrow +\infty$ . Lemma 2 provides a rigorous statement of this property.

**Lemma 2** (Weak ironing).

Let  $f$  be a bounded loss function, let  $\Gamma$  be its graph, and let  $\rho > 0$ . The following holds:

1.  $\Gamma_\rho$  is the graph of a function, which we will denote  $f_\rho$ .
2. If we define  $\Delta(\rho) = \sup f_\rho - \inf f_\rho$ , then  $\Delta(\rho) = \mathcal{O}\left(\frac{1}{\rho}\right)$  as  $\rho \rightarrow \infty$ . More specifically,  $f_\rho - \rho \rightarrow \sup f$  uniformly as  $\rho \rightarrow \infty$ .

*Proof.* 1. Defining  $f_\rho(\theta) = \sup \{y \in \mathbb{R} \mid (\theta, y) \in U\}$ , one verifies with is that the graph of  $f_\rho$  is  $\Gamma_\rho$ .

2. We can rewrite  $f_\rho(\theta)$  as

$$\begin{aligned} f_\rho(\theta) &= \sup_{\theta' \in B(\theta, \rho)} \left[ f(\theta') + \sqrt{\rho^2 - \|\theta' - \theta\|^2} \right] \\ &= \sup_{\|s\| \leq \rho} \left[ f(\theta + s) + \sqrt{\rho^2 - \|s\|^2} \right] \\ &= \sup_{\|s\| \leq \rho} \left[ f(\theta + s) + \rho \sqrt{1 - \frac{\|s\|^2}{\rho^2}} \right]. \end{aligned}$$

Where we have defined  $s = \theta' - \theta$ . As  $\rho \rightarrow +\infty$ , we have the asymptotic expansion

$$\sqrt{1 - \frac{\|s\|^2}{\rho^2}} = 1 - \frac{\|s\|^2}{2\rho^2} + o\left(\frac{1}{\rho^2}\right),$$

which gives the expansion

$$f_\rho(\theta) - \rho = \sup_{\|s\| \leq \rho} \left[ f(\theta + s) + \mathcal{O}\left(\frac{1}{\rho}\right) \right].$$

Finally, we note that as  $\rho \rightarrow +\infty$ ,  $\sup_{\|s\| \leq \rho} f(\theta + s) \rightarrow \sup f$ , which gives the final approximation

$$f_\rho(\theta) - \rho = \sup f + \mathcal{O}\left(\frac{1}{\rho}\right),$$

from which the result follows.

□

This property is demonstrated in Figure 2 for the simple case of the sine function.

A more powerful version of the ironing property does not require the loss function to be bounded. In fact, if two loss functions  $f$  and  $g$  are close, then the RBO should produce similar trajectories on either of them. Furthermore, as the radius of the ball grows, The optimizer can tolerate larger differences between  $f$  and  $g$ .

**Proposition 3** (Strong ironing property).

Let  $f, g : \mathbb{R}^d \rightarrow \mathbb{R}$  be two loss functions, such that  $\|f - g\|_\infty < +\infty$ . Furthermore, let  $\Gamma$ ,  $\Lambda$ ,  $\Gamma_\rho$ , and  $\Lambda_\rho$  be the graphs of  $f$ ,  $g$ ,  $f_\rho$ , and  $g_\rho$  respectively. Then as  $\rho \rightarrow +\infty$ ,  $\Gamma_\rho$  and  $\Lambda_\rho$  become globally isometric.

*Proof.* By Lemma 2, we have that  $f_\rho - \rho \rightarrow \sup f$  and  $g_\rho - \rho \rightarrow \sup g$ , and therefore  $f_\rho - g_\rho \rightarrow \sup f - \sup g$  uniformly as  $\rho \rightarrow +\infty$ . As a result,  $\Gamma_\rho$  and  $\Lambda_\rho$  converge to the same graph (in the Hausdorff metric), up to a vertical translation.  $\square$

This property is particularly useful, since the RBO behaves well for smooth loss functions. Proposition 3 extends this guarantee of good behavior all functions that are close enough to a smooth function.

## 5 Experiments

Having introduced the RBO in Section 3, and established some of its theoretical properties in Section 4, we now examine its behavior empirically. To implement RBO, we used SGD to compute  $\text{proj}_\Gamma$ . Assuming we run  $T$  training epochs, and that each projection uses  $P$  iterations of SGD, we get a runtime on the order of  $\mathcal{O}(T \times P)$ . As such, running extensive experiments on large models and datasets is very time-consuming. As a result, we have limited our experiments to rudimentary cases, deferring more complex evaluations to future work.

### 5.1 Ironing

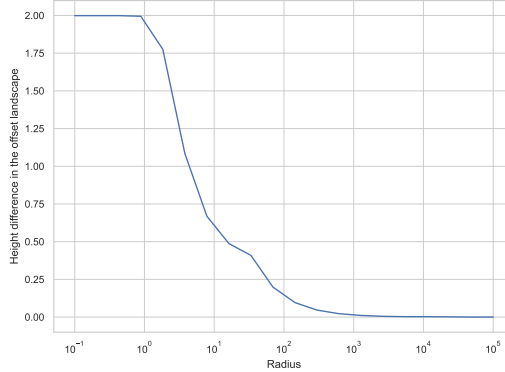


Figure 2: A graph of  $\Delta(\rho)$  for the sine function

To demonstrate the weak ironing property, we computed  $\Delta(\rho)$  for a range of  $\rho$  values, with  $f$  being the sine function on  $[-3\pi, 3\pi]$ . Figure 2 shows the results. We can see that  $\Delta(\rho)$  behaves indeed like  $1/\rho$ , for large  $\rho$ . More interestingly, we observe a plateau for small radii, where every radius below  $\rho = 1$  behaves essentially identically to  $\rho = 0$ . RBO experiences a phase transition at with critical radius  $\rho_c$ . This is in fact a general phenomenon, and in general, the critical radius is given by the *reach* of  $\Gamma$  [11].

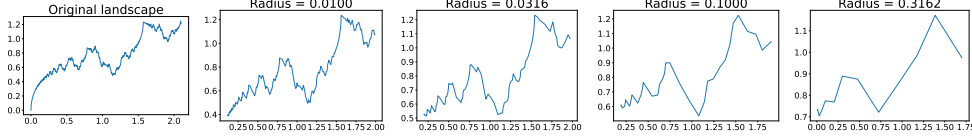


Figure 3: Center trajectory of the RBO for a complicated loss function with  $\theta_0 = 2$ .

As for strong ironing, we test it by running the RBO with a learning rate of  $\eta = 10^{-3}$ , projection step size of  $\gamma = 0.05$ , and projection iteration count of  $P = 20$ , on a loss function given by:

$$f(\theta) = \sum_{k=1}^{100} \frac{\sin(k^2\theta)}{k^2}. \quad (13)$$

The results are shown in Figure 3, where the top left shows the original loss landscape, and each subsequent plot shows the trajectory of RBO with a different value of  $\rho$ . Increasing  $\rho$  results in coarser images of the loss landscape, while maintaining the global shape.

## 5.2 Exploration v.s. Exploitation

Gradient Descent (GD) is fundamentally a greedy algorithm, always taking the immediately optimal step. As a result, it gets easily stuck in local minima. Like most shortcomings we outlined in this paper, this can be traced back to the point-like nature of the update rule. In contrast, RBO can be biased to explore if the radius large, or exploit if the radius small.

To illustrate this divide, we run both SGD and RBO with various radii and from different, but close, initial positions, on the loss function given by

$$f(\theta) = \|\theta\|^2 - \sum_{k=1}^{1000} \exp\left(-\frac{\|\theta - \theta_k\|^2}{\sigma^2}\right), \quad (14)$$

where  $(\theta_k)_{k=1}^{1000}$  are sampled from uniform distribution on  $[-3, 3] \times [-3, 3]$ . Both algorithms are run for 300 iterations, with a learning rate of  $\eta = 0.01$ , while RBO’s projection solver uses  $P = 100$  iterations with step size  $\gamma = 0.001$ .

The results, presented in Figure 4, show that gradient descent was unable to escape the local minimum. Similarly, RBO with small radii ( $\leq 3$ ) was also stuck. On the other hand, RBO with large radii ( $\geq 4$ ) managed to cross the local valley and eventually found the global basin of attraction. In the large radius regime, RBO moves further away from its initial position, covers a larger area of the loss landscape, but exhibits seemingly chaotic behavior. This suggests that large radii may be initially advantageous for finding good basins of attraction, but a transition to a small radius regime is likely necessary to achieve convergence. This is consistent with the “explore early, exploit later” strategy, omnipresent in optimization algorithms.

## 6 Concluding remarks

The point-like nature of the dominant family of optimizers leads to several undesirable properties when the loss landscape is complex, as is often the case in DL. To provide performance guarantees in the presence of challenging geometries, a non-local update rule is required. In this paper, we propose (arguably, the simplest) such an update rule, simulating the motion of a rigid body on the loss landscape. The resulting optimizer has a smoothing effect on the loss landscape, is approximately invariant to small perturbations, and offers explicit control over the trade-off between exploration and exploitation.



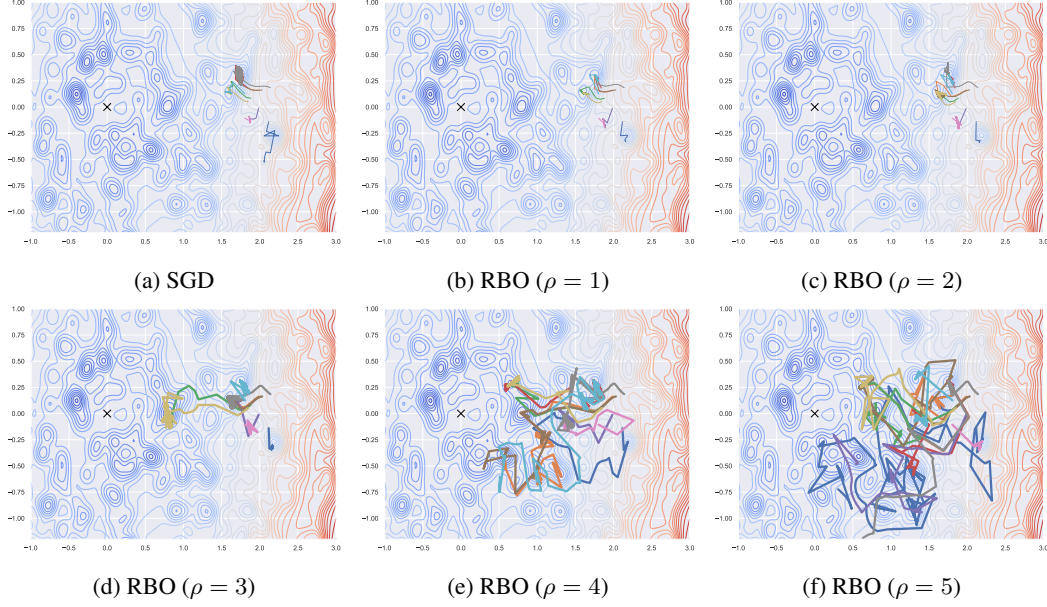


Figure 4: The exploration v.s. exploitation tradeoff for SGD and RBO on a simple loss function. 10 initial positions are shown.

## 6.1 Limitations and future work

While RBOs and non-local optimizers in general are a promising candidate for a truly robust training procedure for deep neural networks (DNNs), much about them remains to be understood, and they are not without their shortcomings.

First, and most pressing, non-local optimizers, including RBO and Entropy-SGD, tend to be significantly more computationally expensive than standard gradient-based optimizers. This complicates large-scale adoption and experimentation. In some cases, like for SAM [8], the non-local update rule can be reduced to a local one, but such a reduction is not always possible.

Second, using an optimization problem as an update rule introduces errors arising from the approximate nature of the solver. These errors can accumulate over time, and are of particular concern given the chaotic early dynamics of RBO with large radii. It is unclear how the dimensionality of the problem influences these errors, but it is not unlikely that the curse of dimensionality exacerbates this problem.

Finally, multiple important questions about RBO in particular, and non-local optimizers in general, remain open. These include:

- Explicit characterization of robustness to data noise. To the extent that the loss landscape is shaped by the data, RBO’s invariance properties imply a form of robustness to data noise, and by extension, better generalization performance. The exact form of this invariance, the degree to which it holds, and its relation to hyperparameters (particularly the radius) are open questions.
- Privacy and poisoning attack robustness. If the answer to the previous question implies that RBO is sufficiently agnostic to the details of the dataset, it is likely to imply both privacy preserving, and poisoning resilience properties, since both families of attacks rely on the assumption that the model is strongly dependent on the data.
- Efficient implementations. Whether it is possible to efficiently approximate RBO with a linear time update rule, and whether such an approximation retains the properties of RBO is still unknown.

## References

- [1] R. Abdulkadirov, P. Lyakhov, N. Nagornov, Survey of Optimization Algorithms in Modern Neural Networks, *Mathematics* 11 (2023) 2466.
- [2] M. Lowell, There is a Singularity in the Loss Landscape, 2022. [arXiv:2201.06964](https://arxiv.org/abs/2201.06964).
- [3] H. Li, Z. Xu, G. Taylor, C. Studer, T. Goldstein, Visualizing the Loss Landscape of Neural Nets, in: *Advances in Neural Information Processing Systems*, volume 31, Curran Associates, Inc., 2018.
- [4] G. Chen, C. K. Qu, P. Gong, Anomalous diffusion dynamics of learning in deep neural networks, *Neural Networks* 149 (2022) 18–28.
- [5] N. S. Keskar, D. Mudigere, J. Nocedal, M. Smelyanskiy, P. T. P. Tang, On Large-Batch Training for Deep Learning: Generalization Gap and Sharp Minima, in: *International Conference on Learning Representations*, 2022.
- [6] S. Hochreiter, J. Schmidhuber, Flat Minima, *Neural Computation* 9 (1997) 1–42.
- [7] Y. N. Dauphin, R. Pascanu, C. Gulcehre, K. Cho, S. Ganguli, Y. Bengio, Identifying and attacking the saddle point problem in high-dimensional non-convex optimization, in: *Advances in Neural Information Processing Systems*, volume 27, Curran Associates, Inc., 2014.
- [8] P. Foret, A. Kleiner, H. Mobahi, B. Neyshabur, Sharpness-aware Minimization for Efficiently Improving Generalization, in: *International Conference on Learning Representations*, 2020.
- [9] P. Chaudhari, A. Choromanska, S. Soatto, Y. LeCun, C. Baldassi, C. Borgs, J. Chayes, L. Sagun, R. Zecchina, Entropy-SGD: Biasing Gradient Descent Into Wide Valleys, 2017. [arXiv:1611.01838](https://arxiv.org/abs/1611.01838).
- [10] L. Chizat, E. Oyallon, F. Bach, On Lazy Training in Differentiable Programming, in: *Advances in Neural Information Processing Systems*, volume 32, Curran Associates, Inc., 2019.
- [11] F. Chazal, D. Cohen-Steiner, A. Lieutier, Q. Mérigot, B. Thibert, Inference of Curvature Using Tubular Neighborhoods, 2017.
- [12] G. Leobacher, A. Steinicke, Existence, uniqueness and regularity of the projection onto differentiable manifolds, *Annals of Global Analysis and Geometry* 60 (2021) 559–587.
- [13] A. Hauswirth, S. Bolognani, G. Hug, F. Dörfler, Projected gradient descent on Riemannian manifolds with applications to online power system optimization, in: *2016 54th Annual Allerton Conference on Communication, Control, and Computing (Allerton)*, 2016, pp. 225–232.
- [14] Sternberg, Biomedical Image Processing, *Computer* 16 (1983) 22–34.